

Can radial motions in the stellar halo constrain the rate of change of mass in the Galaxy?

SANJIB SHARMA,^{1,2} JOSS BLAND-HAWTHORN,^{1,2} JOSEPH SILK,³ AND CELINE BOEHM^{4,5}

¹*Sydney Institute for Astronomy, School of Physics, The University of Sydney, NSW 2006, Australia*

²*ARC Centre of Excellence for All Sky Astrophysics in Three Dimensions (ASTRO-3D), Australia*

³*Institut d'Astrophysique de Paris, 98 bis Bd Arago, Paris, France*

⁴*School of Physics, The University of Sydney, NSW 2006, Australia*

⁵*ARC Centre of Excellence for Dark Matter Particle Physics, Australia*

ABSTRACT

A change in the mass of the Galaxy with time will leave its imprint on the motions of the stars, with stars having radially outward (mass loss) or inward (mass accretion) bulk motions. Here we test the feasibility of using the mean radial motion of stars in the stellar halo to constrain the rate of change of mass in the Galaxy, for example, due to decay of dark matter into invisible dark sector particles or more conservatively from the settling of baryons. In the current Λ CDM paradigm of structure formation, the stellar halo is formed by accretion of satellites onto the host galaxy. Over time, as the satellites disrupt and phase mix, the mean radial motion $\langle V_R \rangle$ of the stellar halo is eventually expected to be close to zero. But most halos have substructures due to incomplete mixing of specific accretion events and this can lead to nonzero $\langle V_R \rangle$ in them. Using simulations, we measure the mean radial motion, $\langle V_R \rangle$, of stars in 13 Λ CDM stellar halos lying in a spherical shell of radius 30 kpc. We find that for most halos, the shell motion is quite small, with 75% of halos having $\langle V_R \rangle \lesssim 1.2 \text{ km s}^{-1}$. When substructures are removed by using a clustering algorithm, $\langle V_R \rangle$ is reduced even further, with 75% of halos having $\langle V_R \rangle \lesssim 0.6 \text{ km s}^{-1}$. A value of $\langle V_R \rangle \approx 0.6 \text{ km s}^{-1}$ can be attained corresponding to a galactic mass loss rate of 2% per Gyr. We show that this can place constraints on dark matter decay parameters such as the decay lifetime and the kick velocity that is imparted to the daughter particle. The advent of all-sky stellar surveys involving millions to billions of stars is encouraging for detecting signatures of dark matter decay.

Keywords: cosmology: dark matter – galaxies: haloes – Galaxy: kinematics and dynamics – Galaxy: halo – Galaxy: formation – Galaxy: structure

1. INTRODUCTION

Dark matter dominates the outer galaxy but may not be absolutely stable. At the very least, this has to be demonstrated to within observational limits. Dark matter is generally considered to consist of weakly interacting particles that are hitherto undetected. Search for observational signatures is a major industry (Feng 2010), including deep underground direct searches (Liu et al. 2017), indirect searches in astronomical systems, including the Universe itself, and high energy particle accelerator searches at the LHC (Kahlhoefer 2017) and elsewhere.

The most popular sought-after signals typically involved self-annihilation of heavy neutral particles into charged Standard Model particles (see e.g., Silk & Srednicki 1984, for the original idea). However many other avenues have been considered as early as in the 1980s, including the decay of dark matter particles, e.g., Dicus et al. (1978); Cabibbo et al. (1981) and Ellis et al. (1984). Decaying dark matter scenarios gained further traction in the past two decades af-

ter puzzling excesses in cosmic ray and X-ray observations emerged, see e.g., Chen et al. (2009); Ibarra & Tran (2009); Yin et al. (2009), or for more modern references von Doetinchem et al. (2020); Carney et al. (2022), as well as Boyarsky et al. (2015); Jeltema & Profumo (2015); Riemer-Sørensen (2016) and references therein. As the injection of charged particles in dark matter halos and our cosmic neighbourhood could lead to excess in cosmic ray, neutrinos, X-ray, gamma-ray and radio spectra, these could be used to set strong limits on the dark matter characteristics and, in particular, constrain its mass vs interaction strength and therefore lifetime.

More recently however it was suggested that dark matter could decay or annihilate into a dark (possibly secluded) sector. While such scenarios would be impossible to detect by traditional means, Abdelqader & Melia (2008); Peter & Benson (2010); Wang et al. (2014) showed that their impact on the number of satellite companions of the Milky Way would provide nonetheless a way to test their validity. More re-

cently, by comparing cosmological simulations of decaying dark matter with the observed Milky Way satellite population [Mau et al. \(2022\)](#) were able to place constraints on the decay lifetime and the associated kick velocity. Here we go a step further and examine whether the invisible dark matter decay would also affect galaxy dynamics and provide complementary limits to previous works, including [Alvi et al. \(2022\)](#).

These questions are more than academic. The Hubble tension (discrepancy between the local measurement of Hubble constant with that from the cosmic microwave background) has reinvigorated discussions about the possible instability of dark energy ([Poulin et al. 2019, 2021](#)) and dark matter ([Pandey et al. 2020; Fernandez-Martinez et al. 2021](#)), but see also [Anchordoqui et al. \(2022\)](#). Models based on either of these hypotheses have the potential of reducing the Hubble tension by modifying the early universe expansion rate relative to its current value.

Another tension where the dark matter decaying scenarios might help is regarding the amplitude of matter fluctuations S_8 between cosmic microwave background (CMB) and gravitational lensing, as the value measured currently is smaller than Λ CDM expectations based on CMB ([Abbott et al. 2018; Abellán et al. 2021](#)). This scenario will be addressed by EUCLID studies of weak lensing ([Hubert et al. 2021](#)). Depending on the results, one might need to invoke new physics in the dark sector and decaying dark matter in particular [Poulin et al. \(2016\)](#).

Here we demonstrate that we can set constraints on both the lifetime and the characteristic kick velocity imparted by the decay from galactic dynamics. The kicks can significantly deplete the dark matter in low mass subhalos and alter the subhalo mass function of Milky Way like galaxies. We measure the radial motion component of halo stars in a specified shell of matter to constrain the change in Galactic mass and constrain the dark matter lifetime.

Hierarchical structure formation within the cold dark matter paradigm is a noisy and complex process. A galaxy with a non-zero rate of change of mass will leave an imprint on the motions of stars within it. Bulk radial motion can be induced directly by the complex orbits of accreting or orbiting material, or by the existence of breathing modes excited by infalling material ([Widrow et al. 2014](#)). A population of stars that, to begin with, are in equilibrium with the Galaxy will drift radially outwards if the mass of the Galaxy decreases, or drift inwards if the mass increases. If the change of potential is slow, and the angular momentum is an adiabatic invariant during this change, then the net average radial motion in a spherical shell is proportional to the radius r of the shell and to the fractional rate of change of mass M enclosed by the

shell ([Loeb 2022](#)),

$$V_R \equiv \frac{dr}{dt} = -\left(\frac{\dot{M}}{M}\right)r \quad (1)$$

$$\approx \left(\frac{\dot{M}/M}{\text{Gyr}^{-1}}\right)\left(\frac{r}{\text{kpc}}\right) \text{ km s}^{-1}. \quad (2)$$

Observationally, this can be detected by measuring the radial velocity of stars in the stellar halo. This offers the possibility to constrain the rate of change of mass in the Galaxy and the processes associated with it, such as the decay of dark matter.

In addition to decaying dark matter, a galaxy can gain or lose mass in a given radius for various reasons, but these are either confined to the inner galaxy or are quite small. In the hierarchical structure formation paradigm, galaxies are formed by accretion and merger events that lead to the growth of their mass with cosmic time. This sudden increase of mass can trigger inward radial motions of stars. However, the fractional rate of change of mass is high in the first 1 – 2 billion years and decreases progressively with time. At late times, feedback from bursty star formation and supermassive black holes can generate an outflow of gas from the central regions of the Galaxy and trigger an outward radial motion of stars ([Pontzen & Governato 2012](#)), but this change is mostly confined to the inner regions of the Galaxy. Galaxies lose mass over billions of years through baryonic radiative processes but the implied radial motion is of order $\langle V_R \rangle \sim 0.03 \text{ km s}^{-1}$ for a Milky Way-sized galaxy ([Loeb 2022](#)).

Stellar halo stars extending up to 100 kpc and beyond ([Helmi 2008](#)) are ideal targets for constraining the rate of change of mass in Milky Way sized galaxies. In order for this to work, the mean radial motion of stellar halo stars in the absence of change in galactic mass should be as close to zero as possible. However it is not clear if that is true. In the current Λ CDM paradigm of structure formation, the stellar halo is formed by accretion of satellites onto the host galaxy ([Bullock & Johnston 2005](#)). Over cosmic time, as the satellites disrupt and phase mix, the mean radial motion of the stellar halo is expected to be close to zero. However, not all satellites are fully phase-mixed and significant substructure can be seen in the Galaxy both in position and velocity space ([Johnston et al. 2008](#)) and this can lead to non zero mean radial motion. The question is how large is it? To answer this, we make use of N-body simulations and investigate the mean radial motion of stars in simulated stellar halos. We compare this with the motion expected in the scenario where dark matter undergoes decay and discuss the physical implications of our results. Finally, we discuss the observational challenges for conducting such a study and if the current and future observational facilities are sufficient equipped to do so.

2. METHODS

In this paper we study the bulk radial motion of stars in the stellar halos and for this we make use of N-body simulations and these are described in Section 2.1. If the stars in the stellar halo are in equilibrium then the mean radial velocity should be zero. However, some accretion events of the stellar halo are not well mixed in phase space and have not reached an equilibrium. These show up as substructures in the phase space and are associated with significant non-zero bulk motion. Since we are interested in the equilibrium component of the stellar halo, we identify and get rid of the substructures using a clustering algorithm. This is described in Section 2.2. For certain halos, although the mean motion of stars in a shell is not zero, the distribution of radial velocities is quite symmetrical about the mean radial velocity. Hence, we devise an alternate scheme to measure the central velocity of stars in a shell and this is described in Section 2.3.

Table 1. Simulated stellar halos. The halos starting with `bj_` are from Bullock & Johnston (2005) while those starting with `fire_` are from Sanderson et al. (2020).

Name	Accretion history	Simulation type
<code>bj_2</code>	ACDM	Idealized
<code>bj_5</code>	ACDM	Idealized
<code>bj_7</code>	ACDM	Idealized
<code>bj_9</code>	ACDM	Idealized
<code>bj_10</code>	ACDM	Idealized
<code>bj_12</code>	ACDM	Idealized
<code>bj_14</code>	ACDM	Idealized
<code>bj_15</code>	ACDM	Idealized
<code>bj_17</code>	ACDM	Idealized
<code>bj_20</code>	ACDM	Idealized
<code>bj_low1</code>	Artificial	Idealized
<code>bj_high1</code>	Artificial	Idealized
<code>bj_rad</code>	Artificial	Idealized
<code>bj_circular</code>	Artificial	Idealized
<code>bj_old</code>	Artificial	Idealized
<code>bj_young</code>	Artificial	Idealized
<code>fire_m12f</code>	ACDM	Cosmological
<code>fire_m12i</code>	ACDM	Cosmological
<code>fire_m12m</code>	ACDM	Cosmological

2.1. Simulated stellar halos

To study the radial velocity of stars in the stellar halo, we make use of N-body simulations. We use three different types of simulations, and these are listed in Table 1. First, is a suite of 10 stellar halos simulated by Bullock & Johnston (2005) (BJ05), named as `bj_X` with $X \in \{2, 5, 7, 9, 10, 12, 14, 15, 17, 20\}$. These have accretion histories derived from a semi-analytical scheme in accordance

with the Λ CDM cosmology. Here, a stellar halo is built up entirely by accretion of satellites. The satellites are modelled by N-body particles evolved individually in an analytical potential. Hence, they are called idealized simulations. Baryons are embedded deep in the inner regions. This is modelled by assigning a mass-to-light ratio to each N-body particle based on its energy, with more tightly bound particles having lower mass-to-light ratio. Second, is a suite of six stellar halos that were simulated by Johnston et al. (2008) (JB08) but with artificial accretion histories, `low1` (made up of predominantly low luminosity satellites), `high1` (made up predominantly high luminosity satellites), `old` (made up of predominantly old accretion events), `young` (made up of predominantly young accretion events), `rad` (made up of accretion events predominantly on radial orbits), `circ` (made up of accretion events predominantly on circular orbits). Except for the accretion history, the JB08 halos are otherwise simulated in the same way as the BJ05. Third, we use 3 Milky Way sized galaxies simulated by the FIRE team (Sanderson et al. 2020; Hopkins et al. 2018; Wetzel et al. 2016), `fire_m12f`, `fire_m12i`, `fire_m12m`. These are state of the art hydrodynamical cosmological simulations including physical processes such as cooling, star formation and feedback.

2.2. Clustering

To identify and remove substructures in the stellar halo, we use the *ENLINK* clustering algorithm (Sharma & Johnston 2009) which will be publicly available ¹. For examples of its application to BJ05 halos see Sharma et al. (2010) and Sharma et al. (2011b). We apply it over the six dimensional (x, y, z, v_x, v_y, v_z) phase-space specified in Cartesian coordinates. The main feature of *ENLINK* that is useful for our application is its ability to identify structures of arbitrary shape and size in any given multidimensional space. Unlike most other clustering algorithms that use a global metric, *ENLINK* makes use of a locally adaptive metric based on the idea of Shannon entropy and calculated using a binary space partitioning tree (Sharma & Steinmetz 2006).

As mentioned earlier, in the BJ05 and JB08 halos each N-body particle has different stellar mass. It is difficult to do clustering analysis on particles with unequal weights. This is because an isolated particle of large weight will spuriously appear as a region of overdensity. Hence, for these halos we use the code GALAXIA (Sharma et al. 2011a) to sample star particles from these simulations. The number of stars spawned by an N-body particle is equal to its total stellar mass divided the mean mass of a star for a given stellar initial mass function (IMF). The main advantage of using GALAXIA is that it samples the stars in the six dimensional

¹ <https://github.com/sanjibs/enlink>

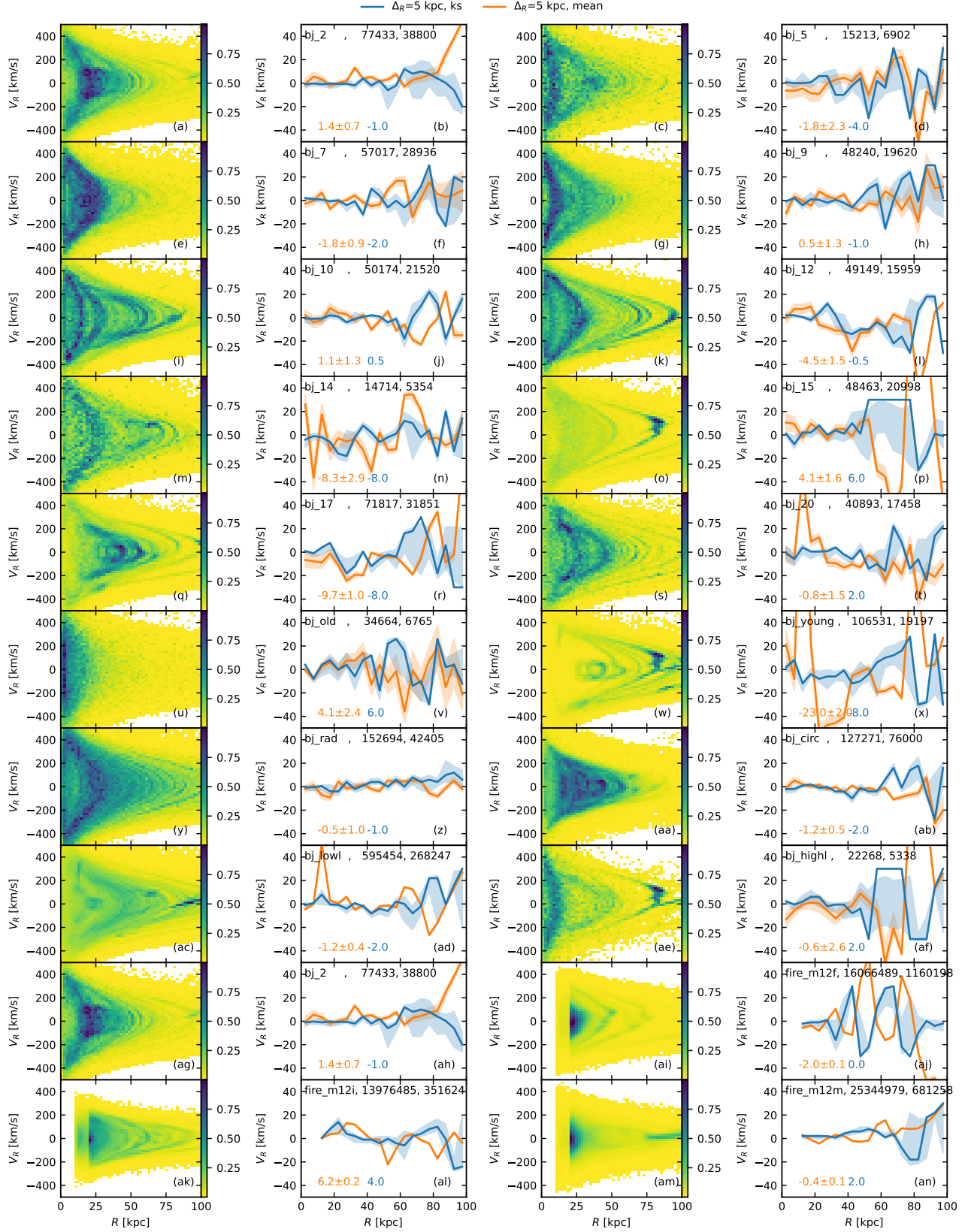


Figure 1. Radial velocity distribution of N-body particles in the stellar halos simulated by (Bullock & Johnston 2005), (Johnston et al. 2008) and (Sanderson et al. 2020). Each N-body particle has a star forming mass associated with them and the distributions are weighted according to them. First and third columns show distribution of stars in (r, V_r) plane in the spherical Galactocentric coordinates. Second and fourth columns show mean radial velocity measured in spherical shells (width 5 kpc) as a function of radius (orange line). Shown alongside (blue line) is the velocity at which the distribution is symmetric. The total number of stars are denoted on the top, followed by number of stars in shell $15 < r/\text{kpc} < 45$. For the same shell, the text at the bottom denotes, mean V_r , the error on the mean and the central velocity based on symmetry.

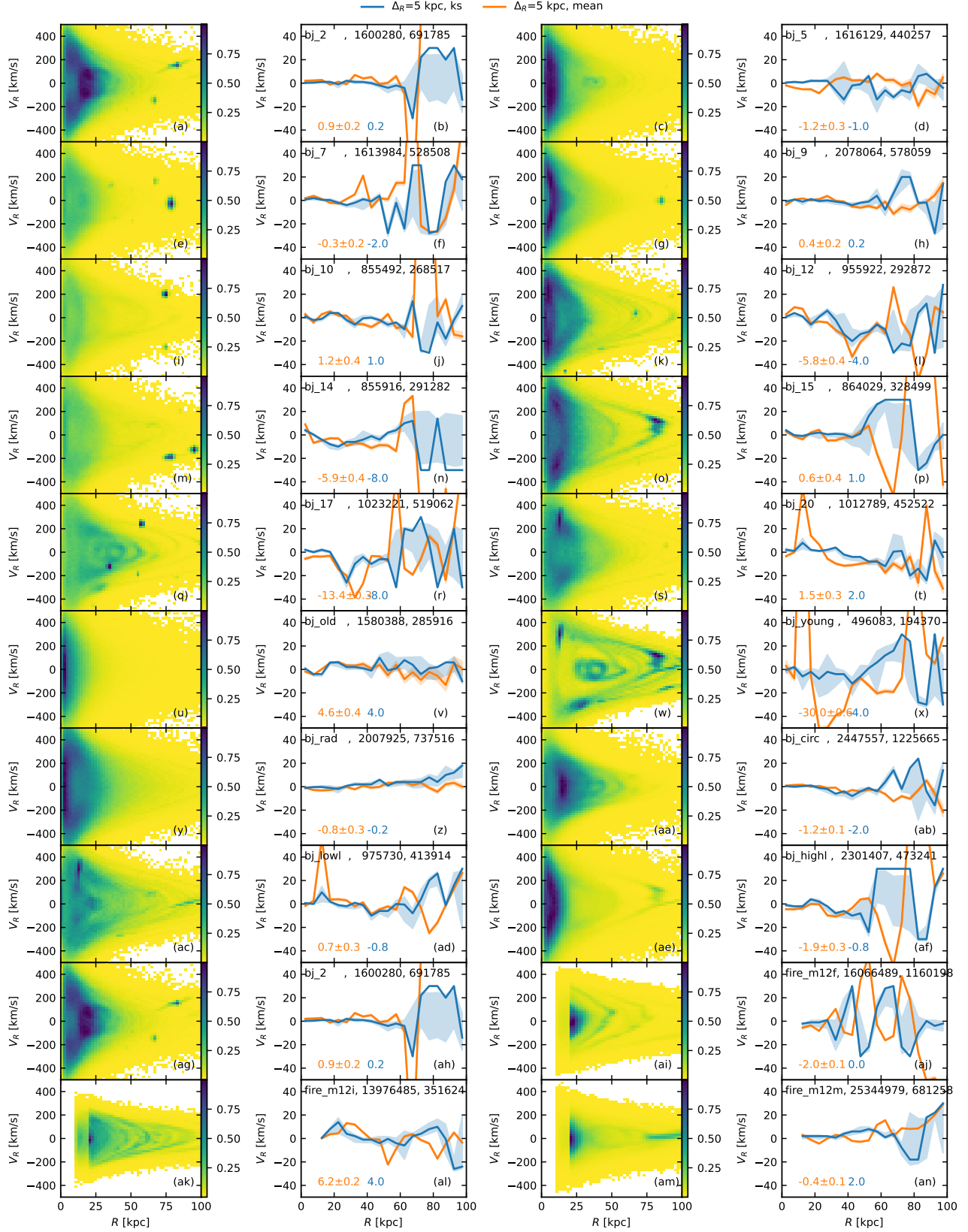


Figure 2. Same as Figure 1 but for equal stellar mass particles. The code *GALAXIA* was used to spawn equal stellar mass particles from N-body particles with a given star forming mass.

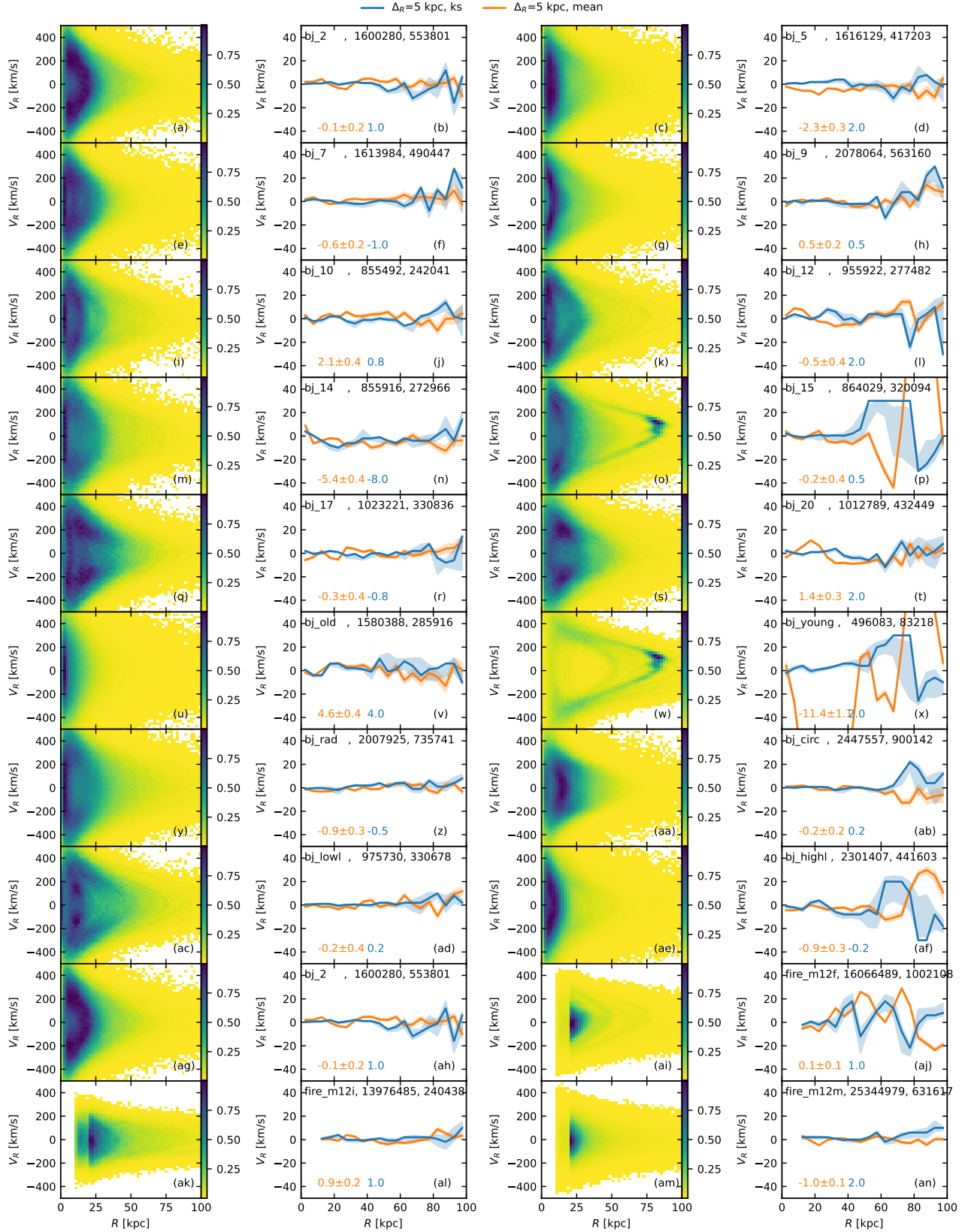


Figure 3. Same as Figure 2 but by filtering out substructures by using the clustering algorithm *ENLINK*.

phase space, hence the sampled stars have kinematics consistent with the original simulation.

2.3. The central radial velocity based on symmetry

For certain accretion events stars are not distributed over the full available phase space of the orbit. This means that at any given r the mean motion is non zero. However, the distribution of radial velocity is symmetrical, and the center of symmetry is close to zero. To compute the central velocity, we divide the sample into two about a chosen center of symmetry. Next, we minimize the the two sample Kolmogorov-Smirnov statistics

$$D_{n,m} = \frac{nm}{n+m} \sup |F_{1,n}(v_r) - F_{2,m}(v_r)| \quad (3)$$

to locate the center of symmetry. Here, $F_{1,n}$ and $F_{2,m}$ are the cumulative distribution function of the first and the second sample, and n and m are the respective number of data points in each of the samples.

3. MEAN RADIAL VELOCITY IN SIMULATED STELLAR HALOS

We begin by studying the radial velocity distribution of simulated stellar halos. Figure 1 shows the distribution of stars in the Galactocentric (r, V_r) space, where r is the radial distance and v_r the radial velocity (panels in first and third columns). Mean radial velocity $\langle V_r \rangle$ measured in spherical shells of width ΔR as function of radius r is shown in panels of second and fourth column (orange line). The central radial velocity, measured as the velocity about which the radial velocity distribution is symmetric, is also shown alongside (blue line). The 16 and 84 percentile spread about the estimated mean and central velocity are denoted by the shaded region. The spread was estimated using the technique of bootstrapping. The mean and central radial velocity for stars in shell $15 < r/\text{kpc} < 45$ is shown in the bottom right of each panel. In Figure 1, for the idealized halos the stars are weighted by the star forming mass of each N-body particle and the bound satellites are removed. Unlike the idealized halo the cosmological halo also has disc stars. To get rid of disc stars, we restrict the analysis to stars with $(R > 20 \text{ kpc})$ or $(|z| > 10 \text{ kpc})$. This is the reason for the vertical streaks at $r = 10 \text{ kpc}$ and $r = 20 \text{ kpc}$ in the *fire* halos.

In Figure 1, significant substructure in the (r, V_r) space can be seen. The mean radial velocity is also found to show significant fluctuations. Next, instead of the N-body particles we repeat the analysis with stellar particles of equal stellar mass spawned by the code *Galaxia*. Results are shown in Figure 2. Bound satellites were not removed and can be seen as dense knots. Substructures are not as clear as before and this is due to two reasons. First, the bound satellites being very dense increase the range of density being mapped by

the color scale, and this lowers the contrast of the less dense substructures. Second, the star spawning process of *Galaxia* also leads to some added scatter of stars in the phase space. In spite of these minor differences, the mean radial profiles are very similar to Figure 1. Next we use the ENLINK clustering algorithm to remove the substructures and retain only the dominant smooth component of the halo. These results are shown in Figure 3. The distribution in (r, V_r) space is much smoother and the mean radial velocity profiles have markedly smaller fluctuations.

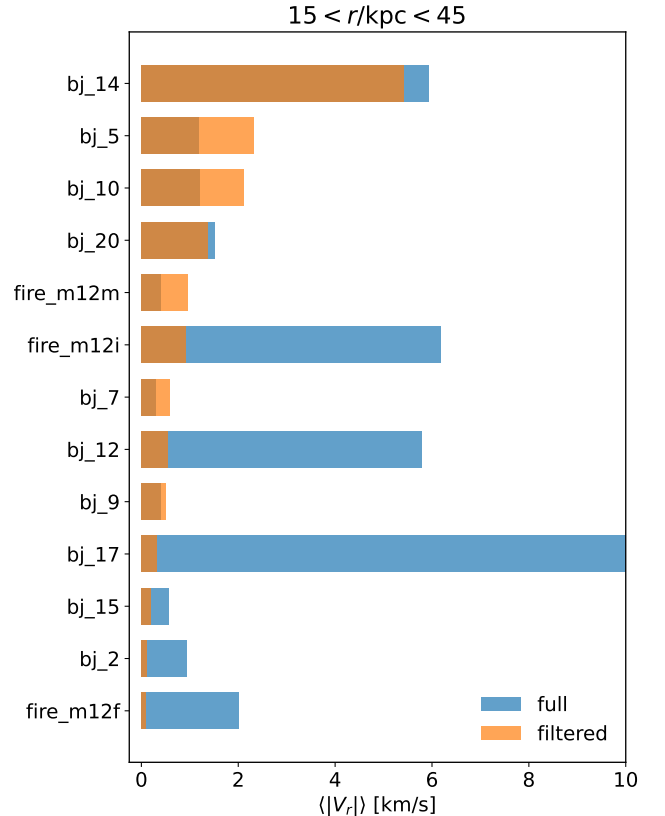


Figure 4. Absolute mean radial velocity of stars in a spherical shell for different simulated Λ CDM stellar halos. Results of the full sample are compared with the sample where substructures were filtered out.

3.1. Mean radial velocity in shell $15 < r/\text{kpc} < 45$.

We now focus on the mean radial velocity in the spherical shell $15 < r/\text{kpc} < 45$ centered around $r = 30 \text{ kpc}$. We choose this radius for the following reasons. From Equation 1 it is clear that the mean radial velocity due to decay is proportional to radius. However, the number density of stars in the Galaxy decreases sharply with radius, making it difficult to find a large number of stars to observe. The density of stars in the stellar halo is well approximated by Hernquist

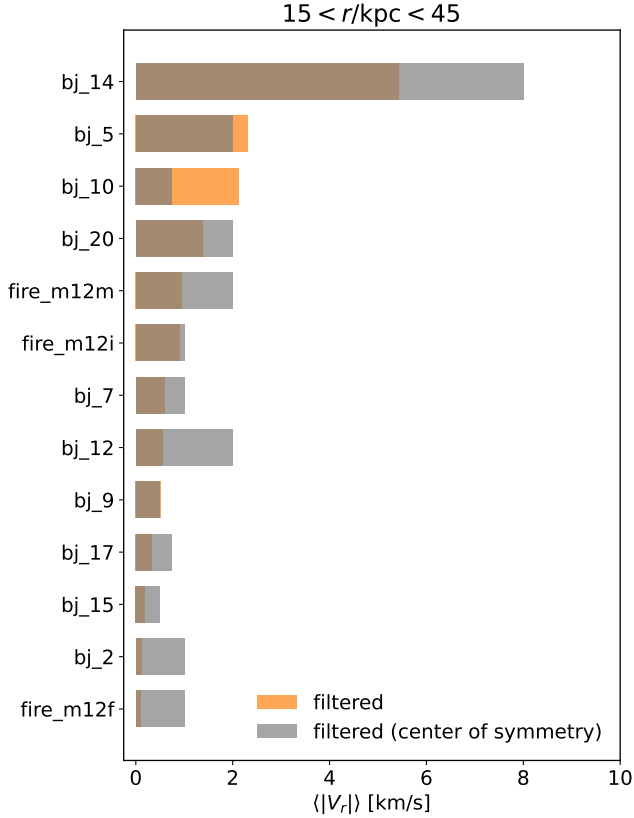


Figure 5. Absolute central radial velocity (see Section 2.3) of stars in a spherical shell for different simulated Λ CDM stellar halos. Results of the full sample are compared with the sample where substructures were filtered out.

profile (Bullock & Johnston 2005), it is high in the center and decreases with radius (varying as r^{-1} at small r and r^{-4} at large r). The further the stars are, the more exposure time is required to observe them. Additionally, the stellar halo is also less phase mixed at large r , which is due to the relaxation time of stars there being large. This can be seen Figure 2 and Figure 3. Finally, for $r < 15$ kpc, the stellar population is dominated by disc stars, which can have significant bulk motion due to non axis-symmetric structures like the spiral arms and the bar. Velocity fluctuations in the disc of the order of 5 to 10 km s^{-1} were shown by (Gaia Collaboration et al. 2018; Khanna et al. 2019a,b). Also the orbiting satellites, like the Sagittarius dwarf galaxy can disturb the disc, an example of this is the (z, V_z) phase space spiral (Antoja et al. 2018; Laporte et al. 2018; Bland-Hawthorn et al. 2019; Laporte et al. 2019).

In Figure 4, we show the shell radial speed using a bar blot for different stellar halos simulated with Λ CDM accretion history. Results for both the full sample and the sample where substructures were filtered out are shown together. Note, we analyse speed instead of velocity. This is to im-

prove the statistics as we only have 13 halos. We assume that mean radial velocity of stars in a shell is equally likely to be either positive or negative. This is very close to true for our sample where the mean velocity of shells was found to be close to zero. It can be seen that for the full sample the shell speed is typically small (median over 13 halos being 1.2 km s^{-1}), but for four halos it is larger than 4 km s^{-1} . After filtering out substructures significant reduction in the speed can be seen, median shell speed being 0.6 km s^{-1} and only one halo having speed above 4 km s^{-1} . This implies that 75% of halos have $\langle V_r \rangle < 0.6 \text{ km s}^{-1}$. In Figure 5 we compare the mean shell radial speed with the central velocity based on symmetry. Although the mean and central radial velocity values differ slightly from halo to halo, but overall the two values are very similar for most halos.

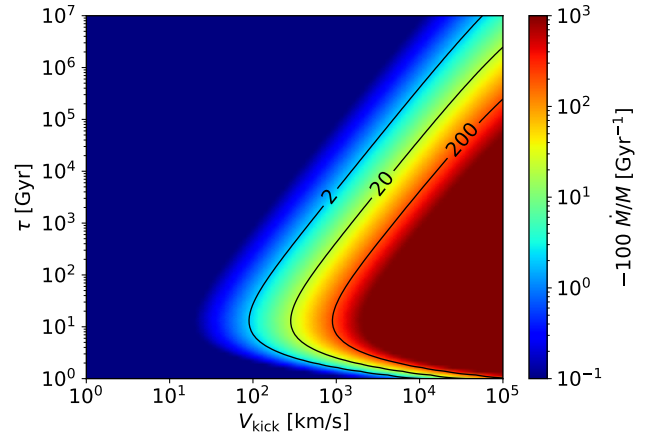


Figure 6. Mass loss rate due to decay of dark matter for a dark matter halo as a function of V_{kick} and decay lifetime τ . Mass loss rate is shown for a sphere of radius 30 kpc and 13 Gyr after the formation of the halo. The solid lines are contours for mass loss rates per Gyr of 2%, 20% and 200%. The result is for an NFW halo with a virial mass of 0.8×10^{12} and concentration parameter $c = 20$, but approximated by a Plummer model following Abdelqader & Melia (2008).

4. IMPLICATIONS FOR DETECTING DARK MATTER DECAY

Dark matter invisible decay is currently unconstrained by dark matter detection experiments both direct and indirect. Here we consider two decay mechanisms and explore if we can detect them using kinematics of stars in the stellar halo. First mechanism is the full decay of a dark matter particle into some form of radiation ($BR = 1$). Second mechanism is the decay into some radiation and a daughter particle lighter than the dark matter. An example of the former scenario is the 2-body decay of the supersymmetric scalar partner of the axion into two axions, where the axions can be dark radiation

(Kawasaki et al. 2008). Examples of the latter scenario include models where the dark matter is coupled to a dark photon/dark Z' (Boehm & Fayet 2004) or, in the case of supersymmetry, sneutrino decaying into a pair neutralino-neutrino or a pair gravitino-neutrino (Kim et al. 2022). These different channels may eventually lead to visible signatures, including in ICECUBE if the dark matter produces high energy neutrinos, but they may also stay invisible for some parts of the parameter space².

In both of the above scenarios, the mass enclosed by a shell of any given radius will decrease with time. In the first scenario there is a direct decrease of mass enclosed by a shell. In the second scenario, the decay imparts a kick to the daughter particle, which induces an expansion of the dark matter halo. In principle, the change of mass can be detected as a non-zero outward radial motion of stars. In Section 3.1, we saw that the median expected radial shell speed of stellar halo at a radius of 30 kpc is 0.6 km s⁻¹. Using Equation 1, this translates to a mass loss rate \dot{M}/M of 0.02 per Gyr. Hence, if the mass loss rate due to decay is higher than 2% per Gyr then it should be detectable using mean motion of stellar halo stars.

The dark matter decay is characterized by the lifetime of decay τ and, in case where there is a daughter particle, the kick velocity V_{kick} imparted to the daughter particle. We now explore in detail the region of the parameter space over which dark matter decay should be detectable using the mean motion of stellar halo stars. In general, for dark matter decaying with lifetime τ the number of unstable dark matter particles N at a time t since the formation of the halo is given by

$$N = N_0 \exp(-t/\tau). \quad (4)$$

and the rate of change by $dN/dt = -N/\tau$. Here, N_0 the initial number of unstable dark matter particles at $t = 0$. For dark matter decaying purely into radiation we have $-\dot{M}/M = 1/\tau$. A limit of $\dot{M}/M > 0.02 \text{ Gyr}^{-1}$ implies $\tau < 50 \text{ Gyr}$.

For the case where dark matter decays into a daughter particle, following previous studies (Abdelqader & Melia 2008; Mau et al. 2022), we assume a dark matter particle χ of mass m decays with lifetime τ into a massive daughter particle χ' of mass m' and a lighter probably massless dark radiation species γ' ,

$$\chi \rightarrow \chi' + \gamma'. \quad (5)$$

Due to conservation of momentum, the decay imparts a velocity kick of

$$V_{\text{kick}} = \epsilon c, \quad (6)$$

where $\epsilon = (m - m')/m$ is the mass splitting factor. The kick increases the velocity dispersion of dark matter particles, which in turn will force the halo to expand. Given the dynamical

time is in general smaller than the decay lifetime, the halo should quickly virialize such that the expansion can be considered to be adiabatic.

Approximating the dark matter halo with a Plummer model, Abdelqader & Melia (2008) derived the increase of its scale radius r_p with time as

$$\frac{dr_p}{dt} = \frac{64r_p^2 c^2}{3\pi GM^2} \frac{\exp[-(t+t_f)/\tau]}{\tau} \times \left[\frac{\chi}{1+\chi} - \left(1 + \frac{3\pi GM}{64c^2 r_p} \right) \frac{\chi(2+\chi)}{2(1+\chi)} \right]. \quad (7)$$

For Plummer model, the mass enclosed by a radial shell is given by

$$M(r) = M_{\text{vir}} \frac{r^3}{(r_p^2 + r^2)^{3/2}} \quad (8)$$

Due to expansion of the dark matter halo, the mass enclosed in a given radial shell should decrease. We estimate this taking the derivative of $M(r)$ with time, which gives

$$\frac{\dot{M}}{M} = \frac{dr_p}{dt} \frac{3r_p}{r_p^2 + r^2}. \quad (9)$$

In Figure 6, we explore the mass loss rate at radius of 30 kpc for a Milky Way mass halo as a function of parameters τ and V_{kick} . Following Abdelqader & Melia (2008) we approximate an NFW halo with a Plummer model, for an NFW halo with scale radius r_s and concentration parameter c the equivalent Plummer scale radius r_p is given by

$$r_p = r_s \frac{3\pi}{16} \left\{ \frac{[\ln(1+c) - c/(1+c)]^2}{1 - 1/(1+c)^2 - 2 \ln(1+c)/(1+c)} \right\}. \quad (10)$$

Figure 6 shows that for $V_{\text{kick}} < 100 \text{ km s}^{-1}$ the mass loss rate per Gyr is less than 2%. However, for $V_{\text{kick}} > 100 \text{ km s}^{-1}$ the rate increases steadily with V_{kick} for any given τ . For a given V_{kick} the mass loss rate seems to be maximum for τ close to 10 Gyr. Contour lines for mass loss rate of 2%, 20% and 200% are shown in the figure. The region of the parameter space over which dark matter decay should be detectable, that is mass loss rate is greater than 2%, can be seen from Figure 6, it is right of the line labelled 2. For a mass loss rate as small as 2% per Gyr, we can rule out for $\tau = 10 \text{ Gyr}$, $V_{\text{kick}} > 100 \text{ km s}^{-1}$. In contrast, a $V_{\text{kick}} \approx 10^4 \text{ km s}^{-1}$ is required to resolve the H_0 tension (Vattis et al. 2019) while a $V_{\text{kick}} \approx 10^5 \text{ km s}^{-1}$ is required to resolve the S_8 tension (Abel-lán et al. 2021). Hence, we are sensitive to values of V_{kick} that are much lower than that required to resolve the tensions of Hubble parameter H_0 and the amplitude parameter S_8 .

Using the observed population of Milky Way satellites Mau et al. (2022) placed constraints of $\tau < 18 \text{ Gyr}$ (29 Gyr) for $V_{\text{kick}} = 20 \text{ km s}^{-1}$ (40 km s⁻¹). This is stricter than the limits that we can set based Milky Way's stellar halo kinematics. This is because the effect of a given kick is stronger

² We disregard $\tilde{G} \rightarrow \chi + \gamma$ as this could be in principle constrained by traditional means.

for smaller subhalos due to their shallower potential wells. However, significant assumptions related to poorly understood baryonic processes are needed in order to connect the subhalos in simulations to luminous satellite galaxies. In this sense our results based on an independent physics are useful and play a complementary role.

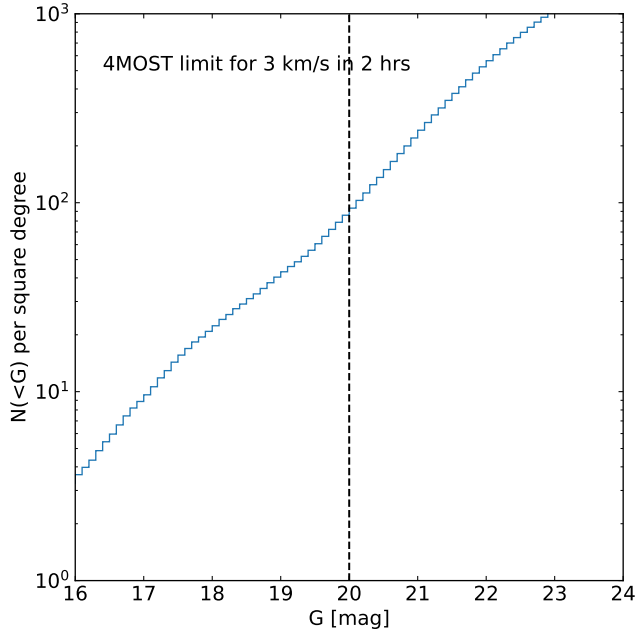


Figure 7. Cumulative number of stars lying in the shell with $(15 < R/\text{kpc} < 45)$ and having $(|z|/\text{kpc} > 10)$, as a function of G band apparent magnitude based on a simulation of the Milky Way by the code *GALAXIA*.

5. OBSERVATIONAL FEASIBILITY

We now look into the feasibility of conducting a study to measure the mean radial motion of Milky Way halo stars in the $15 < r/\text{kpc} < 45$ spherical shell. Two independent arguments suggest that of the order of a million stars would be required to detect mean radial motion of greater than equal to 0.6 km s^{-1} . First, a large sample of halo stars is required to do clustering and filter out substructures, without which the radial motion would be too noisy. Figure 3 shows that of the order of 1 million stars is sufficient to suppress the noise due to substructures. Secondly, to measure a mean motion of 0.6 km s^{-1} , uncertainty of less than 0.1 km s^{-1} is desirable. To achieve this, given that the radial velocity dispersion of stars in the halo is 140 km s^{-1} (Robin et al. 2003), of the order of 1 million stars are required.

Figure 7 shows the cumulative number density of stars lying in shell $15 < R/\text{kpc} < 45$ as a function of G band magnitude based on simulation of the Milky Way by *GALAXIA*. There are close to 90 stars per square degree for $G < 20$. A

multi-object spectroscopic survey in either north or southern hemisphere targeting 10,000 to 15,000 square degrees can easily observe close to a million stars.

We now discuss the exposure time for each pointing and the total duration required to complete a million star survey of halo stars. Given the intrinsic radial velocity dispersion of halo stars is close to 140 km s^{-1} , the requirements on the precision of radial velocity measurements of individual stars are less stringent. Even a precision of $10\text{-}20 \text{ km s}^{-1}$ should be sufficient. Several wide-field surveys have measured stellar radial velocities for millions of stars; these include APOGEE (0.6M, Majewski et al. 2017), GALAH+ (0.6M, Buder et al. 2021), LAMOST (7M, Zhao et al. 2012) and *Gaia* (33M Gaia Collaboration et al. 2021). All of these surveys have been carried out on moderately small telescopes (1-4m diameter) or on mediocre sites, or both, and thus the magnitude limit ($V \lesssim 15$) is too bright for the proposed experiment, yielding a typical measurement accuracy of $1 - 10 \text{ km s}^{-1}$ depending on the survey. With the dawn of wide-field positioners on 8m class telescopes (e.g. PFS on Subaru 8m, WST 12m in Chile), or 4m class telescopes on exceptional sites, e.g. 4MOST on VISTA (de Jong et al. 2019), we are entering a new era where accurate stellar radial velocities will be routinely accessible down to fainter magnitude limits.

We focus on 4MOST for a more detailed study to demonstrate the feasibility of our experiment. This is the next major ESO VLT project, to be delivered by 2025, involving a dedicated optical 4m telescope and multi-object spectrographs. 4MOST can observe 1462 stars at low spectroscopic resolution ($R = \lambda/\delta\lambda \approx 4000 - 7500$) and 812 stars in high resolution ($R \approx 18000 - 21000$) mode. The expected 4MOST limit³ for a 2 hour exposure in low resolution is 1 km s^{-1} (1σ) at $V \sim 18$ increasing to 3 km s^{-1} at $V \sim 20$, which are feasible with proper consideration of which spectral features are not affected by stellar winds (Zwitter et al. 2018). In fact, the 4MOST low-resolution ($R \sim 4000 - 7500$) halo survey (Helmi et al. 2019) is planning to observe almost all halo giants with $G < 20 \text{ mag}$ over 10,000 square degrees, which is about 1.5 million halo stars. Based on *GALAXIA* about one third of these stars (0.5 million) will be in our desired radial shell.

We now estimate the time required for 4MOST if it were to exclusively focus on halo stars that lie in our desired shell. 4MOST has a field of view of 2.5 square degrees, and there are about 225 targets per 4MOST pointing that lie in our desired shell, which 4MOST can easily do given its high multiplexing. With 2 hours of exposures required for a 3 km s^{-1} radial velocity precision, 4MOST can acquire 4 fields per night or about 14,600 square degrees (1.3 million $G < 20$

³ <https://www.4most.eu/cms/facility/overview>

stars in our required shell) in 5 years (assuming 80% of the time available for observations). Given the high multiplexing of 4MOST, one can in principle go fainter to say $G \approx 22$ and try to fill up all 1462 low resolution fibers with stars in our desired shell. However, in this case it is not useful to do so. The 2.5 times increase in exposure time per magnitude cancels the gains due to the increase in target density.

With a view to proposed facilities in the next decade, e.g. the Wide-field Survey Telescope (WST, Ellis et al. 2017), we note that 4MOST is mounted on the VISTA 4m telescope. For the same field of view and fibre density, a 12m class telescope as proposed for the ESO WST can do the above survey about 9 times faster. This remarkable prospect will allow for experiments on external galaxies and many other sophisticated experiments of dark matter properties. With large data sets of halo stars one can also learn about the aspherical nature of the halo as has been shown in simulations, e.g., twisting and stretching of halos (Emami et al. 2021) or the LMC-induced sloshing of the halo (Erkal et al. 2021).

6. CONCLUSIONS

Under the assumption that the stars in the stellar halo are in equilibrium with potential of the Milky Way, there should be no net radial motion of stars. Any change in mass of the Galaxy is predicted to generate bulk radial motion of stars in the galaxy. Hence, a measurement of non zero bulk radial motion puts constraints on the rate of change of mass in the Galaxy. With this in mind, we have studied the expected bulk radial motion of stars in the stellar halo formed in accordance with the currently favoured Λ CDM model of structure formation. Our main result is that the median radial velocity for 75% Λ CDM halos measured in a shell of radius $15 < R/\text{kpc} < 45$ is less than 0.6 km s^{-1} . This implies that using stellar halo stars we can measure the rate of change of

mass provided it is greater than 2% per giga year. If such rate of change of mass is due decay of dark matter purely into radiation then our results suggest that we can detect decay with lifetime of less than 50 Gyr. If the change in mass is due to the decay of dark matter into radiation and daughter particles, then our results suggest that we can detect a decay with kick velocity of the order of 100 km/s and a lifetime of 10 Gyr. If kick velocity is larger than 100 km/s then one can detect decay for a wide range of lifetimes. In order to conduct such an experiment and measure a signal in radial motion of 0.6 km s^{-1} , of the order of 1 million halo stars would be required. This is feasible with the current generation of astronomical facilities like the 4m class 4MOST facility operating over a period of 5 years. Future facilities with a larger telescope aperture can do this even faster.

7. DATA AVAILABILITY

The code GALAXIA used for generating mock observational surveys is available at <http://galaxia.sourceforge.net/>. Links to the stellar halos simulated by BJ05 and BJ07 are also provided there. The galaxies simulated by the fire team are available at <https://fire.northwestern.edu/ananke/>. The code ENLINK used for clustering will be available at <https://github.com/sanjibs/enlink>.

ACKNOWLEDGEMENTS

SS is funded by a Senior Fellowship (University of Sydney), an ARC Centre of Excellence for All Sky Astrophysics in 3 Dimensions (ASTRO-3D) Research Fellowship and JBH's Laureate Fellowship from the Australian Research Council (ARC). JBH is supported by an ARC Australian Laureate Fellowship (FL140100278) and ASTRO-3D.

REFERENCES

- Abbott, T. M. C., Abdalla, F. B., Alarcon, A., et al. 2018, *PhRvD*, 98, 043526, doi: [10.1103/PhysRevD.98.043526](https://doi.org/10.1103/PhysRevD.98.043526)
- Abdelqader, M., & Melia, F. 2008, *MNRAS*, 388, 1869, doi: [10.1111/j.1365-2966.2008.13530.x](https://doi.org/10.1111/j.1365-2966.2008.13530.x)
- Abellán, G. F., Murgia, R., & Poulin, V. 2021, *PhRvD*, 104, 123533, doi: [10.1103/PhysRevD.104.123533](https://doi.org/10.1103/PhysRevD.104.123533)
- Alvi, S., Brinckmann, T., Gerbino, M., Lattanzi, M., & Pagano, L. 2022, arXiv e-prints, arXiv:2205.05636, <https://arxiv.org/abs/2205.05636>
- Anchordoqui, L. A., Barger, V., Marfatia, D., & Soriano, J. F. 2022, *PhRvD*, 105, 103512, doi: [10.1103/PhysRevD.105.103512](https://doi.org/10.1103/PhysRevD.105.103512)
- Antoja, T., Helmi, A., Romero-Gómez, M., et al. 2018, *Nature*, 561, 360, doi: [10.1038/s41586-018-0510-7](https://doi.org/10.1038/s41586-018-0510-7)
- Bland-Hawthorn, J., Sharma, S., Tepper-Garcia, T., et al. 2019, *MNRAS*, 486, 1167, doi: [10.1093/mnras/stz217](https://doi.org/10.1093/mnras/stz217)
- Boehm, C., & Fayet, P. 2004, *Nucl. Phys. B*, 683, 219, doi: [10.1016/j.nuclphysb.2004.01.015](https://doi.org/10.1016/j.nuclphysb.2004.01.015)
- Boyarsky, A., Franse, J., Iakubovskiy, D., & Ruchayskiy, O. 2015, *Phys. Rev. Lett.*, 115, 161301, doi: [10.1103/PhysRevLett.115.161301](https://doi.org/10.1103/PhysRevLett.115.161301)
- Buder, S., Sharma, S., Kos, J., et al. 2021, *MNRAS*, 506, 150, doi: [10.1093/mnras/stab1242](https://doi.org/10.1093/mnras/stab1242)
- Bullock, J. S., & Johnston, K. V. 2005, *ApJ*, 635, 931, doi: [10.1086/497422](https://doi.org/10.1086/497422)
- Cabibbo, N., Farrar, G. R., & Maiani, L. 1981, *Phys. Lett. B*, 105, 155, doi: [10.1016/0370-2693\(81\)91010-8](https://doi.org/10.1016/0370-2693(81)91010-8)

- Carney, D., Raj, N., Bai, Y., et al. 2022, arXiv e-prints, arXiv:2203.06508. <https://arxiv.org/abs/2203.06508>
- Chen, C.-R., Nojiri, M. M., Takahashi, F., & Yanagida, T. T. 2009, *Prog. Theor. Phys.*, 122, 553, doi: [10.1143/PTP.122.553](https://doi.org/10.1143/PTP.122.553)
- de Jong, R. S., Agertz, O., Berbel, A. A., et al. 2019, *The Messenger*, 175, 3, doi: [10.18727/0722-6691/5117](https://doi.org/10.18727/0722-6691/5117)
- Dicus, D. A., Kolb, E. W., & Teplitz, V. L. 1978, *Astrophys. J.*, 221, 327, doi: [10.1086/156031](https://doi.org/10.1086/156031)
- Ellis, J. R., Kim, J. E., & Nanopoulos, D. V. 1984, *Phys. Lett. B*, 145, 181, doi: [10.1016/0370-2693\(84\)90334-4](https://doi.org/10.1016/0370-2693(84)90334-4)
- Ellis, R. S., Bland-Hawthorn, J., Bremer, M., et al. 2017, arXiv e-prints, arXiv:1701.01976. <https://arxiv.org/abs/1701.01976>
- Emami, R., Genel, S., Hernquist, L., et al. 2021, *ApJ*, 913, 36, doi: [10.3847/1538-4357/abf147](https://doi.org/10.3847/1538-4357/abf147)
- Erkal, D., Deason, A. J., Belokurov, V., et al. 2021, *MNRAS*, 506, 2677, doi: [10.1093/mnras/stab1828](https://doi.org/10.1093/mnras/stab1828)
- Feng, J. L. 2010, *ARA&A*, 48, 495, doi: [10.1146/annurev-astro-082708-101659](https://doi.org/10.1146/annurev-astro-082708-101659)
- Fernandez-Martinez, E., Pierre, M., Pinsard, E., & Rosauero-Alcaraz, S. 2021, *European Physical Journal C*, 81, 954, doi: [10.1140/epjc/s10052-021-09760-y](https://doi.org/10.1140/epjc/s10052-021-09760-y)
- Gaia Collaboration, Katz, D., Antoja, T., et al. 2018, *A&A*, 616, A11, doi: [10.1051/0004-6361/201832865](https://doi.org/10.1051/0004-6361/201832865)
- Gaia Collaboration, Brown, A. G. A., Vallenari, A., et al. 2021, *A&A*, 649, A1, doi: [10.1051/0004-6361/202039657](https://doi.org/10.1051/0004-6361/202039657)
- Helmi, A. 2008, *A&A Rv*, 15, 145, doi: [10.1007/s00159-008-0009-6](https://doi.org/10.1007/s00159-008-0009-6)
- Helmi, A., Irwin, M., Deason, A., et al. 2019, *The Messenger*, 175, 23, doi: [10.18727/0722-6691/5120](https://doi.org/10.18727/0722-6691/5120)
- Hopkins, P. F., Wetzel, A., Kereš, D., et al. 2018, *MNRAS*, 480, 800, doi: [10.1093/mnras/sty1690](https://doi.org/10.1093/mnras/sty1690)
- Hubert, J., Schneider, A., Potter, D., Stadel, J., & Giri, S. K. 2021, *JCAP*, 2021, 040, doi: [10.1088/1475-7516/2021/10/040](https://doi.org/10.1088/1475-7516/2021/10/040)
- Ibarra, A., & Tran, D. 2009, *JCAP*, 02, 021, doi: [10.1088/1475-7516/2009/02/021](https://doi.org/10.1088/1475-7516/2009/02/021)
- Jeltema, T. E., & Profumo, S. 2015, *Mon. Not. Roy. Astron. Soc.*, 450, 2143, doi: [10.1093/mnras/stv768](https://doi.org/10.1093/mnras/stv768)
- Johnston, K. V., Bullock, J. S., Sharma, S., et al. 2008, *ApJ*, 689, 936, doi: [10.1086/592228](https://doi.org/10.1086/592228)
- Kahlhoefer, F. 2017, *International Journal of Modern Physics A*, 32, 1730006, doi: [10.1142/S0217751X1730006X](https://doi.org/10.1142/S0217751X1730006X)
- Kawasaki, M., Nakayama, K., & Senami, M. 2008, *JCAP*, 03, 009, doi: [10.1088/1475-7516/2008/03/009](https://doi.org/10.1088/1475-7516/2008/03/009)
- Khanna, S., Sharma, S., Bland-Hawthorn, J., et al. 2019a, *MNRAS*, 482, 4215, doi: [10.1093/mnras/sty2924](https://doi.org/10.1093/mnras/sty2924)
- Khanna, S., Sharma, S., Tepper-Garcia, T., et al. 2019b, *MNRAS*, 489, 4962, doi: [10.1093/mnras/stz2462](https://doi.org/10.1093/mnras/stz2462)
- Kim, J. S., Lopez-Fogliani, D. E., Perez, A. D., & de Austri, R. R. 2022, arXiv e-prints. <https://arxiv.org/abs/2206.04715>
- Laporte, C. F. P., Johnston, K. V., Gómez, F. A., Garavito-Camargo, N., & Besla, G. 2018, *MNRAS*, 481, 286, doi: [10.1093/mnras/sty1574](https://doi.org/10.1093/mnras/sty1574)
- Laporte, C. F. P., Minchev, I., Johnston, K. V., & Gómez, F. A. 2019, *MNRAS*, 485, 3134, doi: [10.1093/mnras/stz583](https://doi.org/10.1093/mnras/stz583)
- Liu, J., Chen, X., & Ji, X. 2017, *Nature Physics*, 13, 212, doi: [10.1038/nphys4039](https://doi.org/10.1038/nphys4039)
- Loeb, A. 2022, *Research Notes of the American Astronomical Society*, 6, 26, doi: [10.3847/2515-5172/ac5185](https://doi.org/10.3847/2515-5172/ac5185)
- Majewski, S. R., Schiavon, R. P., Frinchaboy, P. M., et al. 2017, *AJ*, 154, 94, doi: [10.3847/1538-3881/aa784d](https://doi.org/10.3847/1538-3881/aa784d)
- Mau, S., Nadler, E. O., Wechsler, R. H., et al. 2022, arXiv e-prints, arXiv:2201.11740. <https://arxiv.org/abs/2201.11740>
- Pandey, K. L., Karwal, T., & Das, S. 2020, *JCAP*, 2020, 026, doi: [10.1088/1475-7516/2020/07/026](https://doi.org/10.1088/1475-7516/2020/07/026)
- Peter, A. H. G., & Benson, A. J. 2010, *PhRvD*, 82, 123521, doi: [10.1103/PhysRevD.82.123521](https://doi.org/10.1103/PhysRevD.82.123521)
- Pontzen, A., & Governato, F. 2012, *MNRAS*, 421, 3464, doi: [10.1111/j.1365-2966.2012.20571.x](https://doi.org/10.1111/j.1365-2966.2012.20571.x)
- Poulin, V., Serpico, P. D., & Lesgourgues, J. 2016, *JCAP*, 08, 036, doi: [10.1088/1475-7516/2016/08/036](https://doi.org/10.1088/1475-7516/2016/08/036)
- Poulin, V., Smith, T. L., & Bartlett, A. 2021, *PhRvD*, 104, 123550, doi: [10.1103/PhysRevD.104.123550](https://doi.org/10.1103/PhysRevD.104.123550)
- Poulin, V., Smith, T. L., Karwal, T., & Kamionkowski, M. 2019, *PhRvL*, 122, 221301, doi: [10.1103/PhysRevLett.122.221301](https://doi.org/10.1103/PhysRevLett.122.221301)
- Riemer-Sørensen, S. 2016, *Astron. Astrophys.*, 590, A71, doi: [10.1051/0004-6361/201527278](https://doi.org/10.1051/0004-6361/201527278)
- Robin, A. C., Reylé, C., Derrière, S., & Picaud, S. 2003, *A&A*, 409, 523, doi: [10.1051/0004-6361:20031117](https://doi.org/10.1051/0004-6361:20031117)
- Sanderson, R. E., Wetzel, A., Loebman, S., et al. 2020, *ApJS*, 246, 6, doi: [10.3847/1538-4365/ab5b9d](https://doi.org/10.3847/1538-4365/ab5b9d)
- Sharma, S., Bland-Hawthorn, J., Johnston, K. V., & Binney, J. 2011a, *ApJ*, 730, 3, doi: [10.1088/0004-637X/730/1/3](https://doi.org/10.1088/0004-637X/730/1/3)
- Sharma, S., & Johnston, K. V. 2009, *ApJ*, 703, 1061, doi: [10.1088/0004-637X/703/1/1061](https://doi.org/10.1088/0004-637X/703/1/1061)
- Sharma, S., Johnston, K. V., Majewski, S. R., Bullock, J., & Muñoz, R. R. 2011b, *ApJ*, 728, 106, doi: [10.1088/0004-637X/728/2/106](https://doi.org/10.1088/0004-637X/728/2/106)
- Sharma, S., Johnston, K. V., Majewski, S. R., et al. 2010, *ApJ*, 722, 750, doi: [10.1088/0004-637X/722/1/750](https://doi.org/10.1088/0004-637X/722/1/750)
- Sharma, S., & Steinmetz, M. 2006, *MNRAS*, 373, 1293, doi: [10.1111/j.1365-2966.2006.11043.x](https://doi.org/10.1111/j.1365-2966.2006.11043.x)
- Silk, J., & Srednicki, M. 1984, *Phys. Rev. Lett.*, 53, 624, doi: [10.1103/PhysRevLett.53.624](https://doi.org/10.1103/PhysRevLett.53.624)
- Vattis, K., Koushiappas, S. M., & Loeb, A. 2019, *PhRvD*, 99, 121302, doi: [10.1103/PhysRevD.99.121302](https://doi.org/10.1103/PhysRevD.99.121302)
- von Doetinchem, P., Perez, K., Aramaki, T., et al. 2020, *JCAP*, 2020, 035, doi: [10.1088/1475-7516/2020/08/035](https://doi.org/10.1088/1475-7516/2020/08/035)
- Wang, M.-Y., Peter, A. H. G., Strigari, L. E., et al. 2014, *MNRAS*, 445, 614, doi: [10.1093/mnras/stu1747](https://doi.org/10.1093/mnras/stu1747)

Wetzell, A. R., Hopkins, P. F., Kim, J.-h., et al. 2016, *ApJL*, 827,
L23, doi: [10.3847/2041-8205/827/2/L23](https://doi.org/10.3847/2041-8205/827/2/L23)

Widrow, L. M., Barber, J., Chequers, M. H., & Cheng, E. 2014,
MNRAS, 440, 1971, doi: [10.1093/mnras/stu396](https://doi.org/10.1093/mnras/stu396)

Yin, P.-f., Yuan, Q., Liu, J., et al. 2009, *Phys. Rev. D*, 79, 023512,
doi: [10.1103/PhysRevD.79.023512](https://doi.org/10.1103/PhysRevD.79.023512)

Zhao, G., Zhao, Y.-H., Chu, Y.-Q., Jing, Y.-P., & Deng, L.-C. 2012,
Research in Astronomy and Astrophysics, 12, 723,
doi: [10.1088/1674-4527/12/7/002](https://doi.org/10.1088/1674-4527/12/7/002)

Zwitter, T., Kos, J., Chiavassa, A., et al. 2018, *MNRAS*, 481, 645,
doi: [10.1093/mnras/sty2293](https://doi.org/10.1093/mnras/sty2293)